Atmospheric Research 300 (2024) 107232

Contents lists available at ScienceDirect

Atmospheric Research

journal homepage: www.elsevier.com/locate/atmosres

On collisional drop breakup in orographic rain

Nitig Singh [a], Saurabh Das [a,*], Udaya Kumar Sahoo [b], Shyam Sundar Kundu [b], Swastika Chakraborty [c]

[a] Department of Astronomy, Astrophysics and Space Engineering, Indian Institute of Technology Indore, Indore, 453552, Madhya Pradesh, India
[b] North Eastern Space Applications Centre, Department of Space, Govt. of India, Umiam 793103, Meghalaya, India
[c] Department of Electronics and Communication Engineering, Narula Institute of Technology, Kolkata 700109, West Bengal, India

ARTICLE INFO

Keywords:
Rain drop size distribution
Collisional drop breakup
Orographic rainfall
Z-R relationship
Tropical region

ABSTRACT

Collisional drop breakup is one of the important processes during evolution of the rain drops and leads to modified shape of the drop size distribution (DSD), which is a primary parameter in rain retrieval in remote sensing techniques. Though several experimental and observational studies have been performed in the recent past on this aspect, the impact of the same in natural rain, particularly in orographic rain, is still poorly represented. The present study aims to examine and identify the rain conditions in which collisional drop breakup is prominent and is capable of modifying the shape of DSD in orographic rain over north-eastern India. The 2-min averaged DSDs from four hilly locations are studied in both stratiform and convective rain types separately using ground-based DSD measurements. Even though drop breakup in intense to moderate rain seemed to be in notable percentage (0.2% - 11.2%), the low intensity rain also showed a considerable break-up signature (2.5% - 9%), depending upon the locations. The overall results showed that collisional breakup was more prominent in convective rain (1%–11%) than in stratiform rain (4%–5%), however, breakup is also seen primarily during stratiform rain in two of the locations. The *Z*-R coefficients are found to be significantly different for the break-up and non-break up cases. For breakup cases, both convective and stratiform rainfall shows an increase in intercept parameter for all locations. For stratiform rain types, the coefficient a and b ranged from 307.6 to 321.4 (167.1–178.7) and 1.27–1.37 (1.31–1.34) for rain with break-up (without break-up), respectively. In the case of convective rain, the coefficients were found to be in the range of 377.5–654.7 (270.4–641.3) and 1.28–1.42 (1.14–1.31) with break-up (without break-up), respectively. The results suggest that collisional breakup is an important process in orographic rain over North-Eastern India and it has to be taken care of, while studying rainfall over these regions, particularly in conventional radar derived quantitative precipitation estimates (QPE).

1. Introduction

Rainfall is a form of precipitation that occurs when water vapor in the atmosphere condenses and falls to the Earth's surface. Raindrops usually form through the ice phase in the atmosphere, except in the case of warm clouds where they form directly from water droplets. Orographic rainfall occurs when moist air is forced to rise over mountains eventually cooled and condensed into clouds. The windward side of mountains is typically the wettest, as this is where the air rises the most. Orographic rainfall can be either convective or stratiform. The boundary between convective and stratiform rainfall is not always clear in orographic rainfall regions. This is because even in a stable environment, strong updrafts (>1 m per second) can occur, depending on the wind and the topography.

Convective rainfall prevails in warm, tropical regions due to favorable conditions for thunderstorm formation, while mid-latitudes experience more stratiform rainfall, attributed to cooler and less moist air. However, studies in the eastern tropical Atlantic, northern Australia, and western equatorial Pacific reveal a strong association between convection and stratiform rain events (Houze, 1993; Houze, 1997). Stratiform rainfall occurs when a large air mass rises and cools slowly, forming nimbostratus clouds producing light to moderate rain, often linked to frontal systems, orographic lifting, or high-pressure systems (Pruppacher et al., 1980).

The altitude, terrain, topography, local weather conditions, rain types, and seasons all influence the microphysical description of different types of rainfall, which is commonly quantified in terms of drop size distribution DSD (Das et al., 2009; Kadiri et al., 2023). Both

* Corresponding author.
E-mail addresses: das.saurabh01@gmail.com, saurabh.das@iiti.ac.in (S. Das).

https://doi.org/10.1016/j.atmosres.2024.107232
Received 30 August 2023; Received in revised form 16 November 2023; Accepted 7 January 2024
Available online 12 January 2024

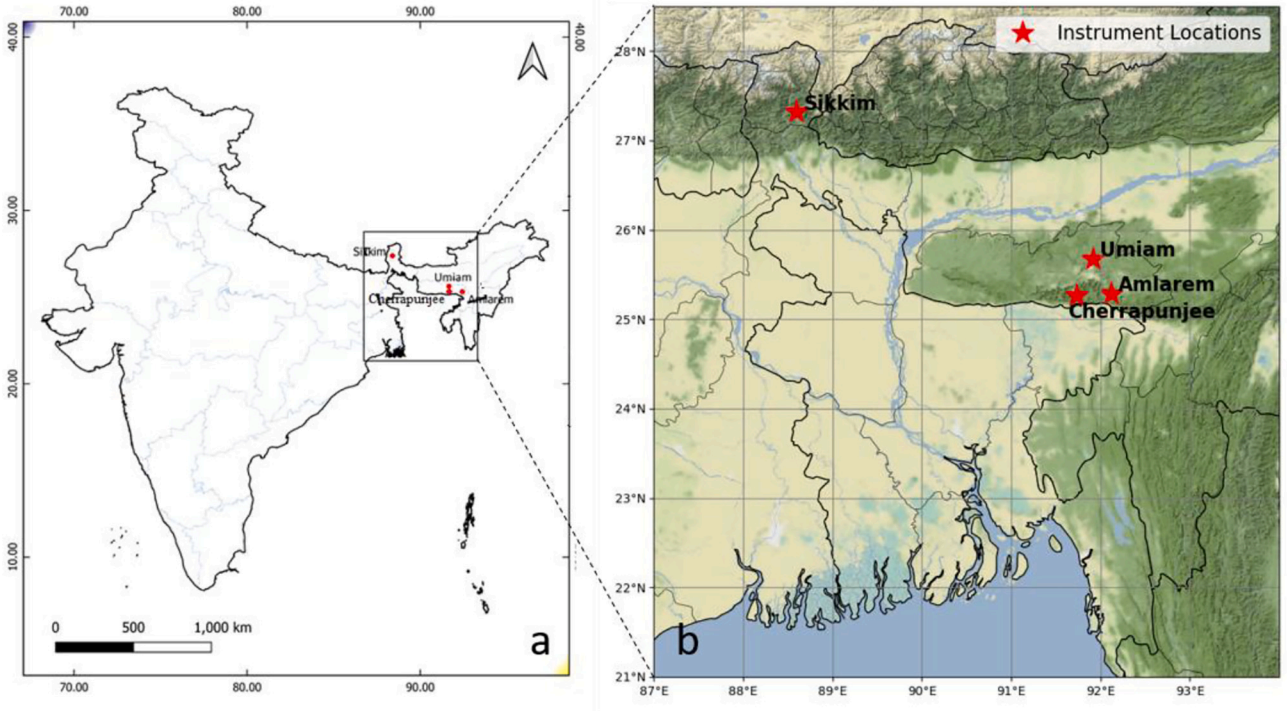

Fig. 1. a) Location and b) Topographic map of the four observation sites over North-East India.

Table 1
Monthly data availability for the four location datasets according to the year of observation. Here cross represents missing data and data available are represented with ticks on it.

LPM (YEAR)/Months	January	February	March	April	May	June	July	August	September	October	November	December
Amlarem (2022)	✓	✓	✓	✓	✓	✓	✓	✓	✓	✓	✘	✘
Cherrapunjee (2022)	✓	✓	✓	✓	✓	✓	✓	✓	✓	✓	✘	✘
Sikkim (2021)	✓	✓	✓	✓	✘	✘	✓	✓	✓	✓	✓	✓
Sikkim (2020)	✘	✘	✓	✓	✓	✓	✓	✓	✓	✓	✓	✓
Umiam (2019)	✘	✘	✘	✘	✓	✓	✓	✓	✓	✘	✘	✘
Umiam (2018)	✘	✘	✓	✓	✓	✓	✓	✘	✘	✘	✘	✘
Umiam (2017)	✘	✘	✘	✘	✓	✓	✓	✓	✓	✓	✓	✘

Table 2
2-min processed observation for each LPM datasets categorized by convective and stratiform rain types for drop breakup study.

LPM Station	Measurement period (Year)	Total 2-min Samples	Convective rain type 2-min samples	Stratiform rain type 2-min samples	Observed Precipitation in the period (mm)
Amlarem	1	30,322	6853	23,469	10,368
Sikkim	2	22,421	712	21,709	2059
Umiam	3*	28,920	2133	26,787	4198
Cherrapunjee	1	31,542	7985	23,557	10,808

* Samples for only rainy season.

stratiform and convective rain, exhibits distinct DSD patterns, with stratiform rain having a narrow-peaked distribution while convective rain displaying a wider range of drop sizes (Pruppacher et al., 1980; Tokay and Short, 1996; Houze, 1993). Seasonal variations, such as warmer temperatures and higher atmospheric instability in summer, also found to influence DSD, with warmer seasons generally associated with larger drops (Pruppacher et al., 1980). Orographic rains are also influenced by many other factors (Caracciolo et al., 2008). Higher altitudes result in colder and drier air, leading to smaller drops (Bringi et al., 2003). Complex terrain and mountainous areas can cause orographic lifting and turbulence, affecting DSD by altering wind speed and causing drop breakup (Pruppacher et al., 1980; Kumjian and Prat, 2014; D'Adderio et al., 2018; Kadiri et al., 2023). Local weather conditions, including temperature, humidity, atmospheric instability and wind patterns also impact drop formation and its evolution. (Pruppacher et al., 1980; Tokay and Short, 1996; D'Adderio et al., 2018).

Collisional drop breakup is an important process in the formation of rain (D'Adderio et al., 2015). The DSD shapes and characteristics are also varied due to collisional drop breakup during its vertical evolution in natural rain (Gillespie and List, 1978; Kumjian and Prat, 2014; Chatterjee et al., 2022; Barthes and Mallet, 2023). Collisional drop breakup is a process that occurs when two water drops collide with each other. The collision can cause the small drops to break into smaller droplets, or it can cause the larger drops to deform. The type of breakup that occurs rely on a number of aspects, which includes the size and speed of the drops, the surface tension of the water, and the presence of

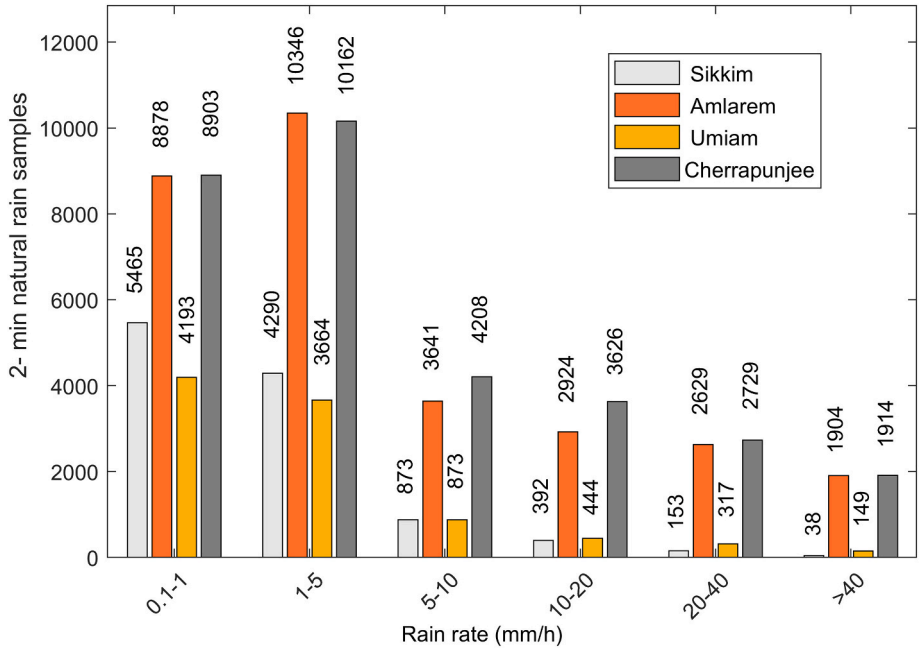

Fig. 2. Distribution of rain rates (mm/h) in all four locations.

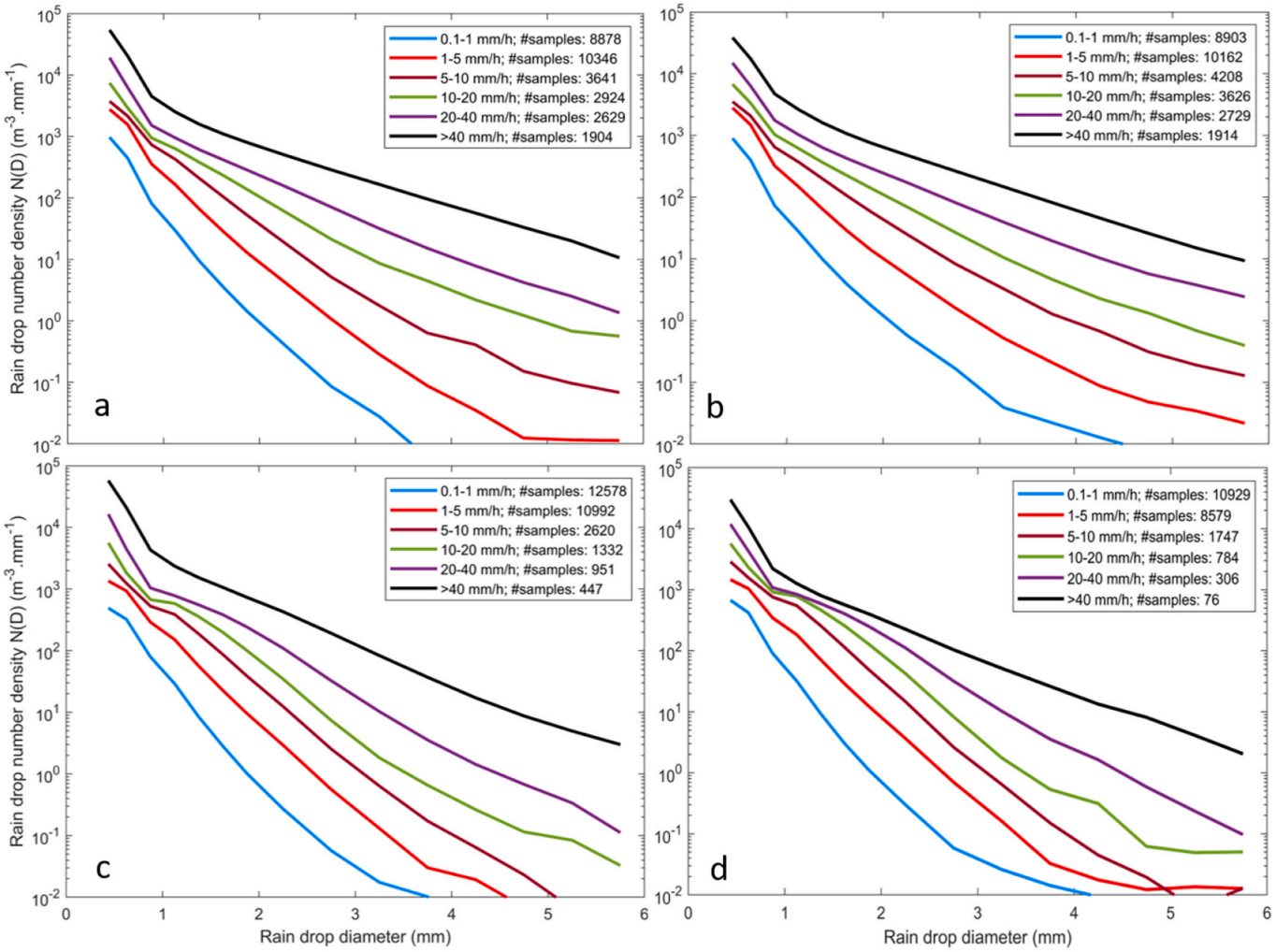

Fig. 3. Mean DSDs for 6 different rainfall rate ranges for (a) Amlarem, (b) Cherrapunjee, (c) Umiam and (d) Sikkim.

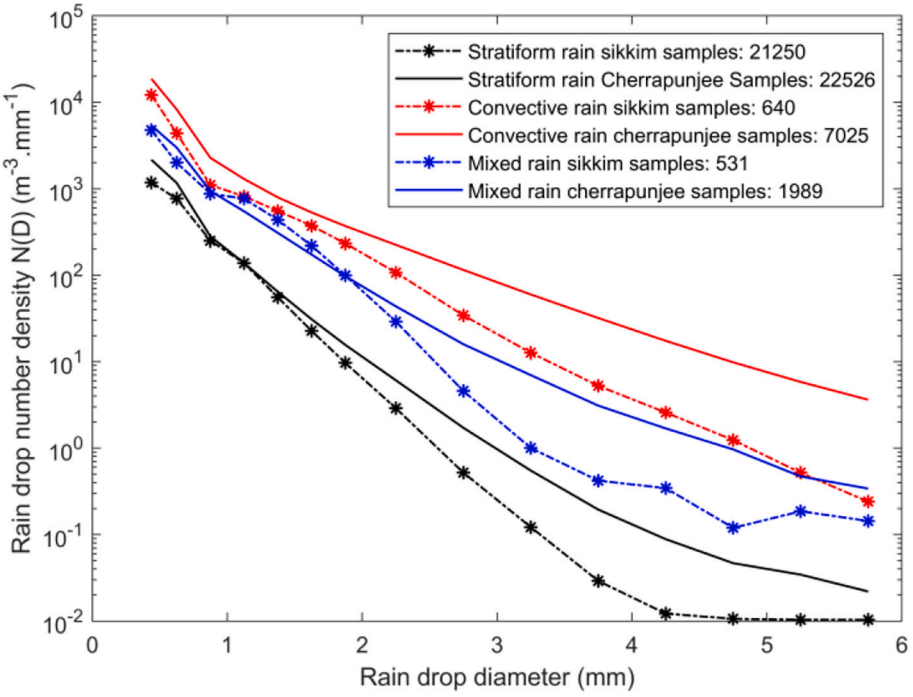

Fig. 4. Mean DSDs of stratiform, convective and mixed rain types in Sikkim with dashed star line and Cherrapunjee with continuous line.

any impurities in the air (List and Gillespie, 1976, Cotton and Gokhale, 1967).

In the early 1960s, experiments were conducted in a vertical wind tunnel to study the collision and breakup of large water drops. In the 1970s, a theoretical model was developed for collisional drop breakup based on the assumption that the breakup of a drop was caused by the tensile stress that was created when the drop was deformed by the impact of another drop, this model was able to predict the breakup of drops with a high degree of accuracy (List and Gillespie, 1976). The phenomena of collisional breakup of drops was initially studied (Brazier-Smith et al., 1972), and later it was investigated in more detail (Low and List, 1982, Valdez and Young, 1985). Various investigations have tackled the parameterization of raindrop collision-induced breakup through laboratory experiments, impacting numerical rain models and size distribution. Computer simulations to solve the stochastic equation explaining evolution of DSD show that the condensation, coalescence, and break up of drops within clouds produce an inverse exponential distribution of drop sizes. (McFarquhar, 2004). However, a comprehensive theoretical depiction of resulting fragment size distributions remains elusive (McFarquhar, 2004). Consideration of drop eccentricity and spatial distribution is crucial in modeling raindrop collisions accurately (Schlottke et al., 2010). Studies on raindrop growth and breakup in warm rain underscore the importance of multiple cycles, regrowth time for breakup fragments, and updraft strength influence (Johnson, 1982). Theoretical regime diagrams have outlined various outcomes of binary raindrop collisions, offering insights into associated physical conditions (Testik et al., 2011). Comparisons of microphysical properties between tropical and temperate locations reveal differences in drop concentrations, with tropical sites showing higher concentrations of medium and large drops. These studies also indicate the occurrence of drop breakup and coalescence in natural rain at both tropical and temperate locations (Gillespie and List, 1978; Longkumer et al., 2023).

The process of collisional breakup of raindrops is intricate and can occur due to various factors including collisions between raindrops, ice breakup, the coexistence of ice and supercooled water, overlapping rain shafts and the complex interplay of all these mechanisms (Radhakrishna and Narayana Rao, 2009). For breakup to occur, the collision kinetic energy (CKE) must exceed 5 mJ (D'Adderio et al., 2015; Low and List, 1982). The most effective breakup occurs when a raindrop of approximately 1.5 mm collides with a larger drop exceeding 3 mm. While breakup between larger raindrops is possible, it is less common (Schlottke et al., 2010). Collisional breakup can cause the DSD to become more spread out, with more raindrops at smaller diameter.

The ground measurements of DSD can be useful to understand the rain evolution process as it captures the signature of the origin and the process involved in collisional drop breakup and drop coalescence. As Multimodal DSD are considered a prominent signature for both the above-mentioned microphysical processes, although collisional breakup is identified by multipeaks in a specific range of drop diameter (D'Adderio et al., 2015). Multimodal DSD can be observed in all types of rain regimes, with variations in the magnitudes of their occurrences along with seasonal variations (Radhakrishna and Narayana Rao, 2009, Konwar et al., 2022). Observations and measurements conducted at different elevations have been instrumental in estimating the occurrence of breakup in real rainfall events and enhancing our understanding of terminal velocities and raindrop sizes during breakup events (Schlottke et al., 2010). Moreover, the analysis of large datasets of DSD using automated algorithms has revealed that dominant breakup and modification of DSDs are rare in natural rain. Further detailed analyses are suggested to better comprehend the conditions under which breakup is more likely to be dominant in rain formation (D'Adderio et al., 2015; Porcù et al., 2013).

The current work studied the local rain microphysics over four hill station of North-Eastern India and investigates the collisional breakup in natural rainfall, for various rain types. The impact of collision drop break up on DSD shape, and consecutively on the *Z*-R relationships were also investigated. The paper is organized as follows: Section 2 outlines the study site, data, the instrument used, and the methodology followed. Section 3 highlights the results and their discussion, followed by the study's conclusions, which are summarized in Section 4.

2. Location, data and methodology

2.1. Location and data

Data used for the present study is obtained from four geographic

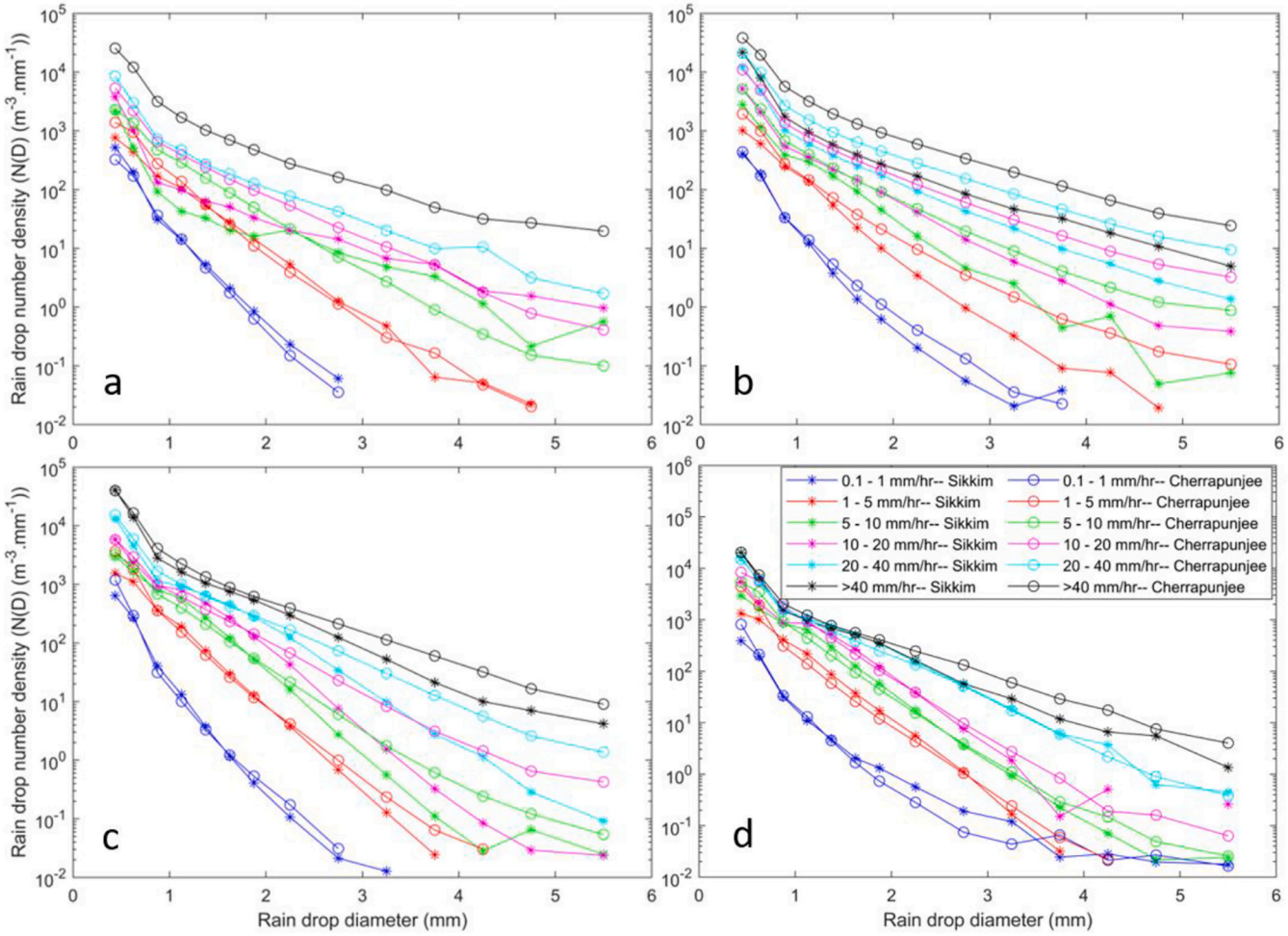

Fig. 5. Mean DSDs of Sikkim and Cherrapunjee for 6 different rainfall rates for various seasons (a) DJF: Winter, (b) MAM: Pre-Monsoon, (c) JJAS: Monsoon, (d) ON: Post Monsoon. Star and circle represent Sikkim and Cherrapunjee, respectively, whereas color represents the different rain intensities.

locations namely, Sikkim (SK) (27° 10′ 58", 88° 30' 06", 351 m), Umiam (UM) (25° 40′ 25.32", 91° 54' 47.52", 1068 m), Cherrapunjee (CH) (25° 16′ 7.500", 91° 44' 0.944", 1296 m) and Amlarem (AM) (25° 17′ 9.96", 92° 7' 10.56", 1034 m) in the north-eastern hilly region of Himalayas. Fig. 1 shows the spatial variation of the locations. Umiam, Amlarem and Cherrapunjee lies within 26 km radius whereas Sikkim lies farthest, almost 400 km away from the three locations.

The rain DSD is measured by a laser precipitation monitor (Clima, 2022) with 1-min temporal resolution at each location. The instruments at Umiam, Cherrapunjee and Amlarem were maintained by North Eastern Space Application Center, Umiam, Meghalaya, whereas the measurements for Sikkim are taken by Sikkim Manipal Institute of Technology, Sikkim.

The instrument measures the particle sizes and velocities that fall within the limits of 22 particle size (0.16 – >8 mm) and 20 velocity ranges (0.2 – >10 m. s^{-1}). The measurement principal is based on the reduction of the power of a light beam that is transmitted from one end of the disdrometer to the other. The magnitude and time of this reduction determine the size and velocity of the passing particle (Thies. 2022).

Northeast India stands out as the region in India that receives the highest amount of rainfall. This can be attributed to its geographical features, which encompass hilly areas, proximity to the Himalayas and Bay of Bengal. Due to these factors, orographic effects play a crucial role in determining the rainfall patterns observed in northeast India. The onset of monsoons in this region takes place in June, marking the beginning of a period characterized by substantial rainfall that lasts from June to September with some rainfall in pre-monsoon (March–May) and post monsoon (October–November) (Murata et al., 2020). July is the wettest month in most of the places.

Umiam, is located in a hilly region with wet tropical climate with average rainfall around 2980 mm. Cherrapunjee, located on the southern slope of the Meghalaya Plateau, northeast India receives about 11,478 mm of average annual rainfall (Kalita et al., 2021). It also holds the record for the highest rainfall observed in a single calendar month, with an astounding 9300 mm recorded in July 1861. Additionally, the town also set a record for the highest rainfall received over a 12-month period, measuring 26,461 mm between August 1, 1860, and July 31, 1861 (Murata et al., 2020). Amlarem is located 42 km east of Cherrapunjee, however, receive an average rainfall of 5966 mm during the mid-May to September. Sikkim is in the northeastern part of the country and receives 3580 mm of annual average rainfall.

The raw data obtained was found to have some missing measurements as given in the Table 1. A data quality pre-processing step was performed on the raw 1-min rainy samples to enhance the accuracy and reliability of subsequent analysis and also prevent the potential failure of the algorithm.

Data quality pre-processing involved following steps:

i. DSD is considered up to 6 mm diameter. The bigger drops >6 mm is unrealistic in rain.
ii. Samples having no particles in the diameter bin class above 6 (1.0 mm) are removed.
iii. 2 min averaging was done on the samples for stabilized DSD (D'Adderio et al., 2015).

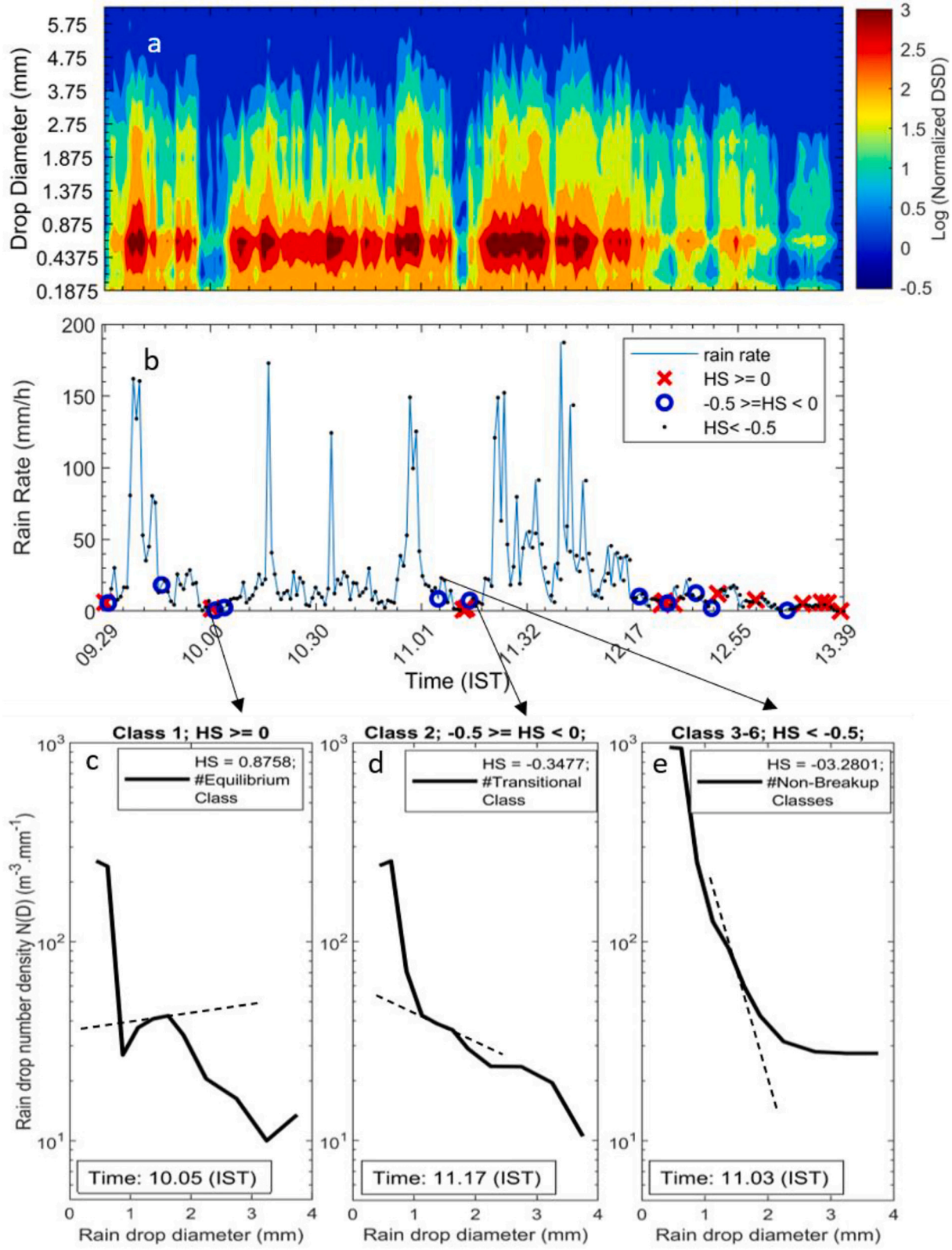

Fig. 6. Case study for the rainfall event in Cherrapunjee from 0929 to 1339 IST 26 March 2022, where (a) shows the time series of the drop size distribution (DSD), (b) rain rate timeseries indicating occurrences of different types of DSD (Equilibrium DSD: red cross and Transitional DSD: blue circle and Non breakup DSD (black dots)) and (c, d, e) depicts the comparison of the mean DSD shape with different values of HS of the linear fit (in dashed lines), where, (c) showing the DSD for equilibrium class (Class 1), (d) showing the DSD for Transitional class (Class 2) and (e) is showing DSD of Non breakup classes. (For interpretation of the references to color in this figure legend, the reader is referred to the web version of this article.)

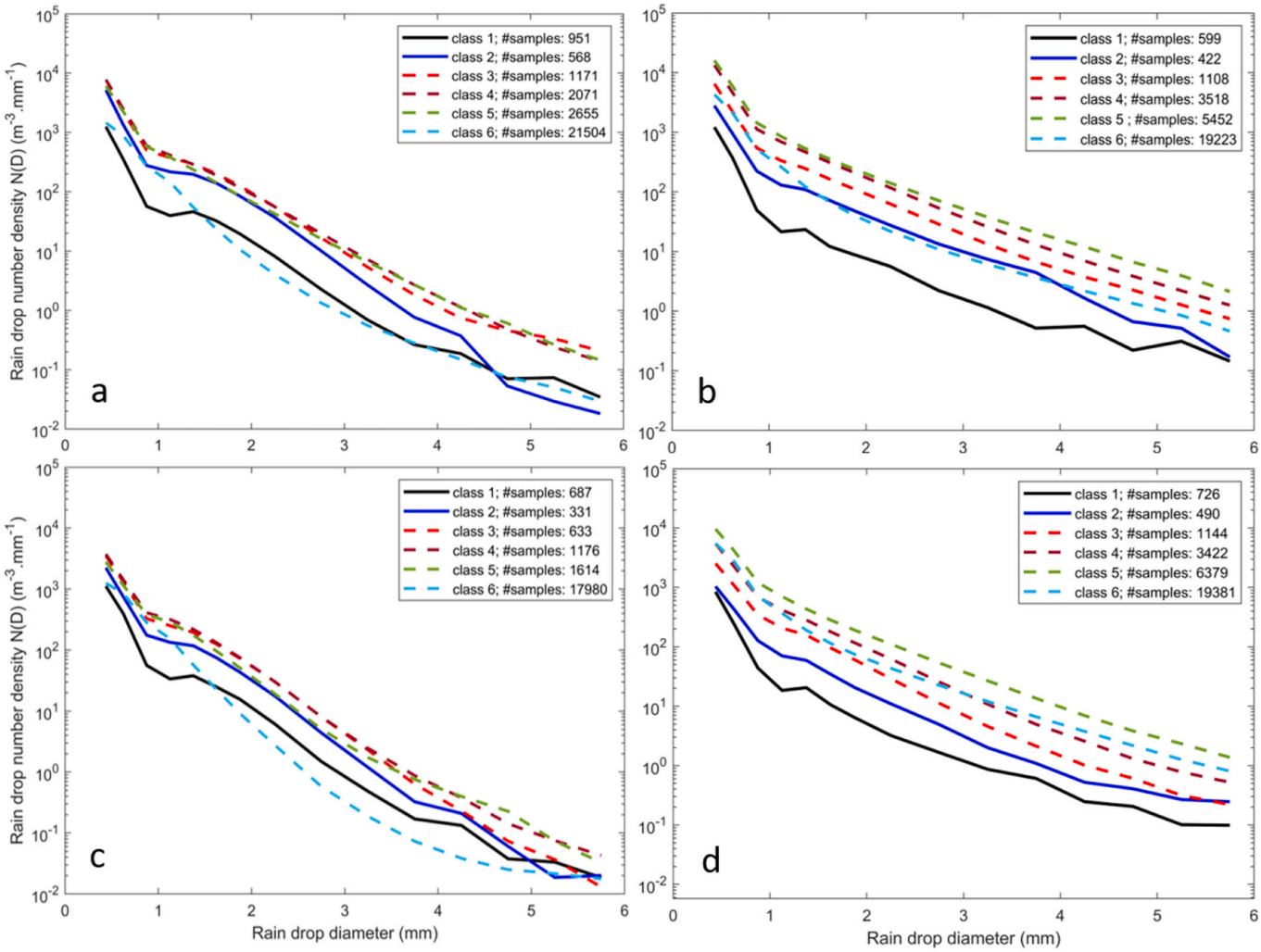

Fig. 7. Mean DSD for each HS class obtained from LPM data for (a) Umiam, (b) Amlarem, (c) Sikkim and (d) Cherrapunjee, highlighting the breakup dominant classes (class 1 (Equilibrium class): black color and class 2 (Transitional class): blue color). (For interpretation of the references to color in this figure legend, the reader is referred to the web version of this article.)

iv. A minimum rainfall threshold of 0.1 mm/h is adopted to eliminate spurious rain samples.
v. A further filter is applied to data set, excluding those drops with measured velocity out of the ±50% interval with respect to Gunn and Kinzer velocity, in order to minimize outliers. (Adirosi et al., 2023).

2.2. Methodology

The processed 2-min samples used for further analysis are categorized into convective and stratiform rain types based on the conditional range of radar reflectivity value. Convective types of rain were assumed when the radar reflectivity is over 38 dBZ while stratiform types were indicated with reflectivity values below 38 dBZ (Tokay and Short, 1996; Das et al., 2009). This, however, means both heavy stratiform and shallow convective are not separately considered, which is often part of mixed types of rain. Table 2 shows the processed 2 min samples categorized by rain type (convective and stratiform).

The presence of breakup can be identified by analyzing the slope of the DSD. For the same, a breakup identification algorithm (D'Adderio et al., 2015) based on Highest Slope (HS) is designed. When breakup is dominant, the DSD shows a characteristic signature, an inflection point in the DSD between 1.0 and 2.6 mm. The inflection point represents a transition from a positive to a negative slope in the DSD and is caused by a reduction in number of raindrops around 1.5 mm in diameter due to breakup. Additionally, breakup leads to an increase in smaller drops (<1 mm in diameter) and an increase in drops around the 2–3 mm range. This phenomenon contributes to the formation of multiple peaks in the DSD (D'Adderio et al., 2015).

The algorithm consists of five interconnected steps. It starts by calculating the linear best fit for the DSD between 1.0 and 2.6 mm. Four different starting points within 1.0 to 1.6 mm are considered, resulting in four linear relationships. The Highest Slope (hereafter referred as HS) value from these fits is used as a reference to label the DSD. The DSDs are then sorted based on the HS values which helps identify patterns. Finally, six classes are defined based on the specific range of HS values as discussed in the case study in result section.

Previous studies indicated that the occurrence of breakup is prominent during both light and heavy rainfall events (Valdez and Young, 1985; Zawadzki and Antonio, 1988; Saikranthi et al., 2023). Hence, the DSD samples <1 mm/h were retained as the percentage breakup in the range could not be neglected. The estimation of the percentage occurrence for classes 1 and 2 in optical disdrometers is often underestimated. This underestimation is primarily due to the wider width of the DSD bins used by the instrument. The wider bins result in a smoother DSD curve, which makes it challenging to identify and capture a significant portion of breakup cases. This limitation in the instrument's characteristics hinders the accurate recognition and representation of breakup events in

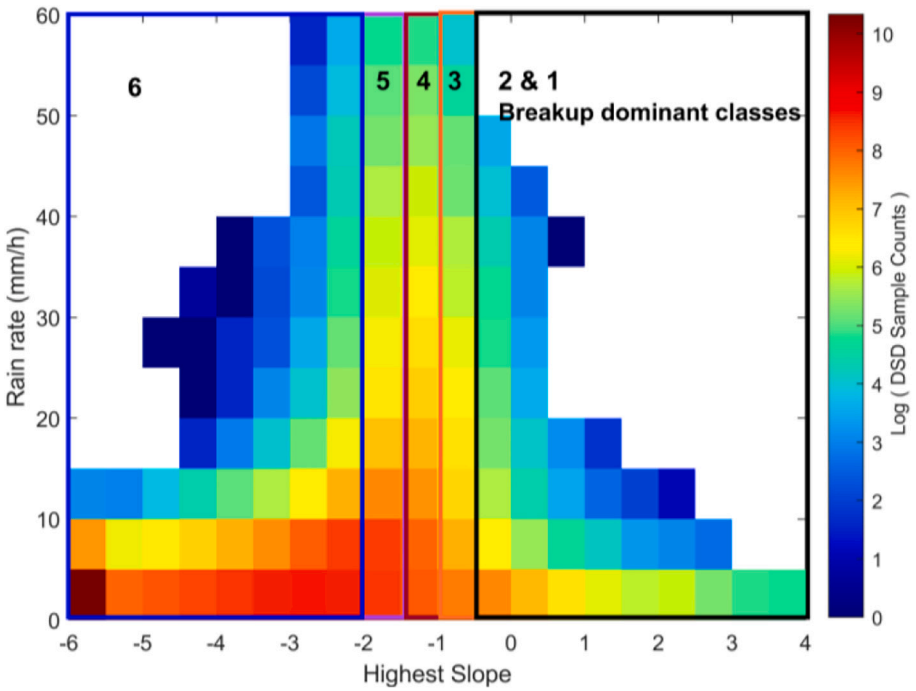

Fig. 8. Distribution of 2-min DSD samples with variation of rain intensity in 6 classes of Highest Slope (HS), highlighting the breakup dominant DSDs in class 1 and class 2.

Table 3
The percentage occurrences of breakup dominant HS class 1 & 2 of total 2-min DSD observation for various rain rate for each LPM Station.

Station	Umiam		Sikkim		Cherrapunjee		Amlarem	
Rain Rate (mm/h)	% Class 1 DSDs	% Class 2 DSDs	% Class 1 DSDs	% Class 2 DSDs	% Class 1 DSDs	% Class 2 DSDs	% Class 1 DSDs	% Class 2 DSDs
0.1–1	4.9	1.4	4.5	1.4	6.1	2.5	5.0	2.1
1–5	2.0	1.5	1.5	1.3	1.5	1.8	1.2	1.3
5–10	1.8	2.6	2.1	1.7	0.4	1.1	0.5	0.9
10–20	3.2	4.6	1.9	2.3	0.4	0.7	0.4	1.2
20–40	2.7	8.5	2.9	7.5	0.1	0.4	0.1	0.8
> 40	0.2	4.2	0	0	0.1	0.1	0.1	0.4

the recorded data (Johannsen et al., 2020; Pickering et al., 2019). Hence, it may lead to overestimation of breakup in experimental raindrop size distributions (DSDs) at lower intensities and hence, a filter of 0.1 mm/h is used to minimize the effect, as shown in step (iv) of Data quality pre-processing. Further, instrument bias, also results in skewed drop size distributions, overestimating small droplets and underestimating large ones during heavy rain (Johannsen et al., 2020; Pickering et al., 2019). The relatively high concentration of smaller-size drops is primarily attributed to the overestimation of small drops by Thies LPM (Tokay et al., 2013). Thus, the first two bins with very high concentrations are omitted. While the overestimation of small droplets is concerning, however, is not affecting our study significantly as our focus is primarily on the 1.0 and 2.6 mm diameter range for the breakup study.

In general, the rain estimation in radar remote sensing employs *Z*-R relationship. Theoretically, the statistical moments of the recorded DSDs are related to the rain rate R (mmh^{-1}) and the radar reflectivity factor Z (mm^6m^{-3}). The Z-R relationships in the study were determined using the least squares approach between the logarithms of Z and R to see the effects of collisional breakup. Each measured DSD is classified in to break -up or non-break-up classes based on the HS slope of the DSD. Then the Z-R relations are estimated separately for stratiform rain and convective rain.

3. Results and discussions

3.1. The local rain micro-physics

Total 113,205 two-minute DSD samples combining all the four locations were analyzed in present study. The Fig. 2 shows the annual average number of 2 min samples for different rain rate ranges. It indicates that the lowest rain rate between 0.1 and 1 mm/h has the highest frequency of rain samples and the number decreases with increase in rain rate. Amlarem and Cherrapunjee has a higher frequency of rain samples for all rain rates compared to other locations as seen in Fig. 2. Specially, Amlarem experienced very heavy rain fall for the period considered for study as seen in the observed precipitation in Table 2.

Figure 3 shows the variation of number of raindrops per unit volume per diameter range, N(D) ($m^{-3}.mm^{-1}$) with raindrop size, D (mm), for rain rate classes with ranges 0.1–1 mm/h, 1–5 mm/h, 5–10 mm/h, 10–20 mm/h, 20–40 mm/h and rain rate beyond 40 mm/h for all locations. The contribution of concentration of small drops (< 1 mm diameter) is predominant for all locations and all rain rate classes.

The large drop concentrations in Cherrapunjee and Amlarem is higher than the Sikkim and Umiam, for rain rate above 5 mm/h. The maximum drop size reaches upto 3.6 mm in 0.1–1 mm/h rain in Amlarem and Umiam whereas it goes beyond 4.5 mm in case of Sikkim. There are multipeaks seen in intermediate rain rates in Sikkim and Umiam around 1 mm drop diameter indicating transition of collisional

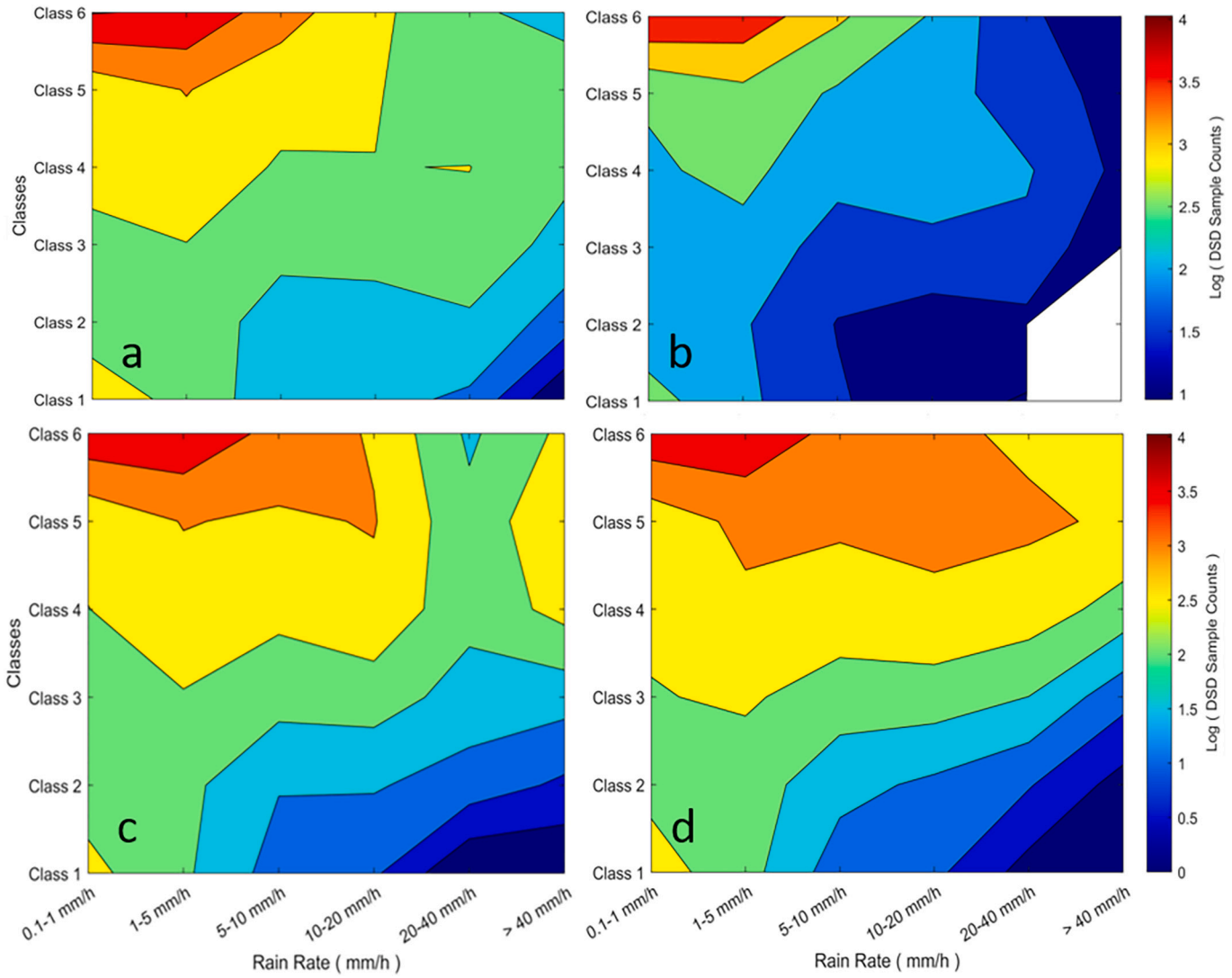

Fig. 9. Distribution (logscale) of 2-min DSD observations for each class variation with rain intensity ranges for (a) Umiam, (b) Sikkim, (c) Amlarem and (d) Cherrapunjee.

process into equilibrium stage. The analysis revealed that Sikkim and Umiam shows similar rain microphysical characteristics while other two locations, Cherrapunjee and Amlarem exhibiting similar rain characteristics. Thus, only Cherrapunjee and Sikkim were further analyzed to understand the rain type and seasonal variation as shown in Figs. 4 and Fig. 5 respectively. Cherrapunjee and Sikkim are both located in the eastern Himalayas, but Cherrapunjee is at a higher altitude than Sikkim. This difference in altitude means that the two locations experience different weather conditions, which may affect the DSD (Zeng et al., 2022; Kundu et al., 2023). Another reason for choosing Cherrapunjee and Sikkim for this study is the sufficient availability of data.

Figure 4 shows the DSD characteristics based on type of rain. The categorization into convective and stratiform rain types based on the conditional range of rain rate and radar reflectivity values (Das and Maitra, 2018; Das et al., 2009). When the rain rate (R) is <10 mm/h and the reflectivity factor (Z) is <38 dB, it indicates strong stratiform rain. On the other hand, when the rain rate is >10 mm/h and the reflectivity factor is >38 dBZ, it signifies strong convection. In cases where the rain rate is >10 mm/h and the reflectivity factor is <38 dBZ (indicating heavy stratiform rain), or when the rain rate is <10 mm/h and the reflectivity factor is >38 dB (indicating shallow convective rain), it combinedly implies a mixed rain type (Das and Maitra, 2018; Caracciolo et al., 2008). Typically, convective rain is characterized by high rain rates and a higher concentration of large raindrops as shown in Fig. 4 for Sikkim and Cherrapunjee. Sikkim exhibits steeper slope of DSD curve, in comparison to Cherrapunjee for all rain types.

The seasonal variation of DSDs is shown in Fig. 5 indicating the general shape of the DSD is similar for all locations. The DSD tends to be more flatten as the rain rate rises, indicating a wider range of drop sizes with high drop concentration. With increased rain rates, there is also a discernible change in the concentration of the distribution toward bigger drop sizes. Both the locations showed varied difference in DSDs for various rain rate classes in the winter season, although higher intensity rain samples were not registered in Sikkim for this period. In general, both the locations show significant seasonal variation of DSDs in all rain rate ranges.

3.2. An investigation on collisional-drop breakup

3.2.1. Identification and occurrences of collisional-drop breakup

A very high rainfall event was observed on March 25–26, 2022 in Cherrapunjee with total rainfall of about 438 mm. In Fig. 6, An example rainfall event is shown that occurred from 0929 to 1339 IST on March 26, 2022. Fig. 6(a), shows the time series of the DSD providing a

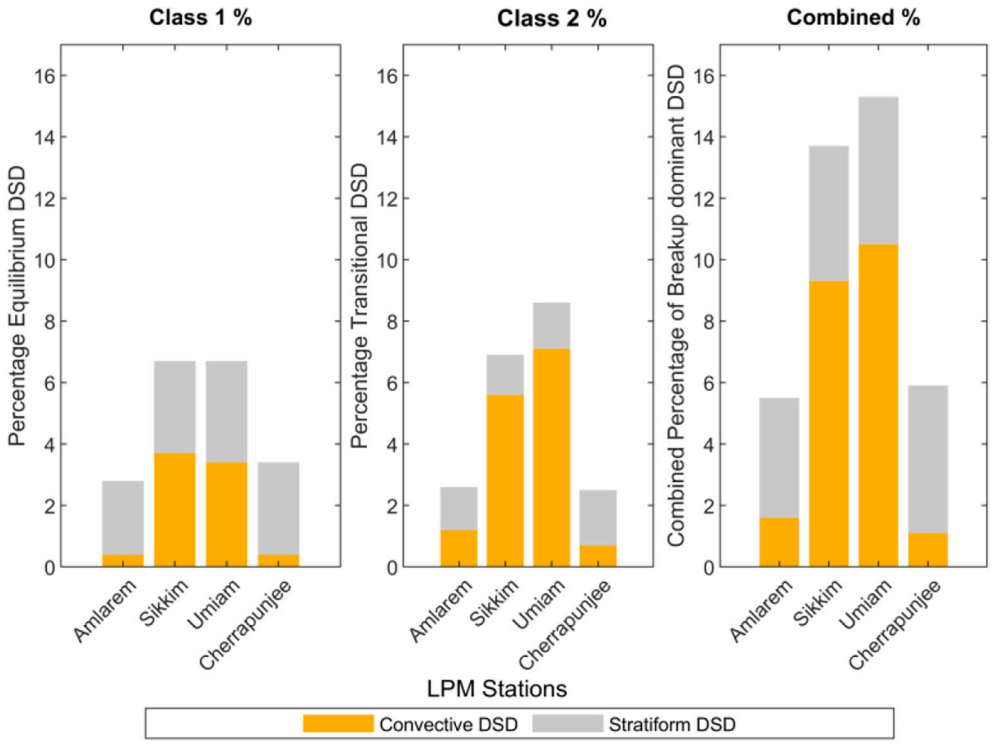

Fig. 10. Class 1, Class2 and total combined percentage of occurrences of breakup in the 2-min DSD for convective and stratiform rain samples in the four study locations.

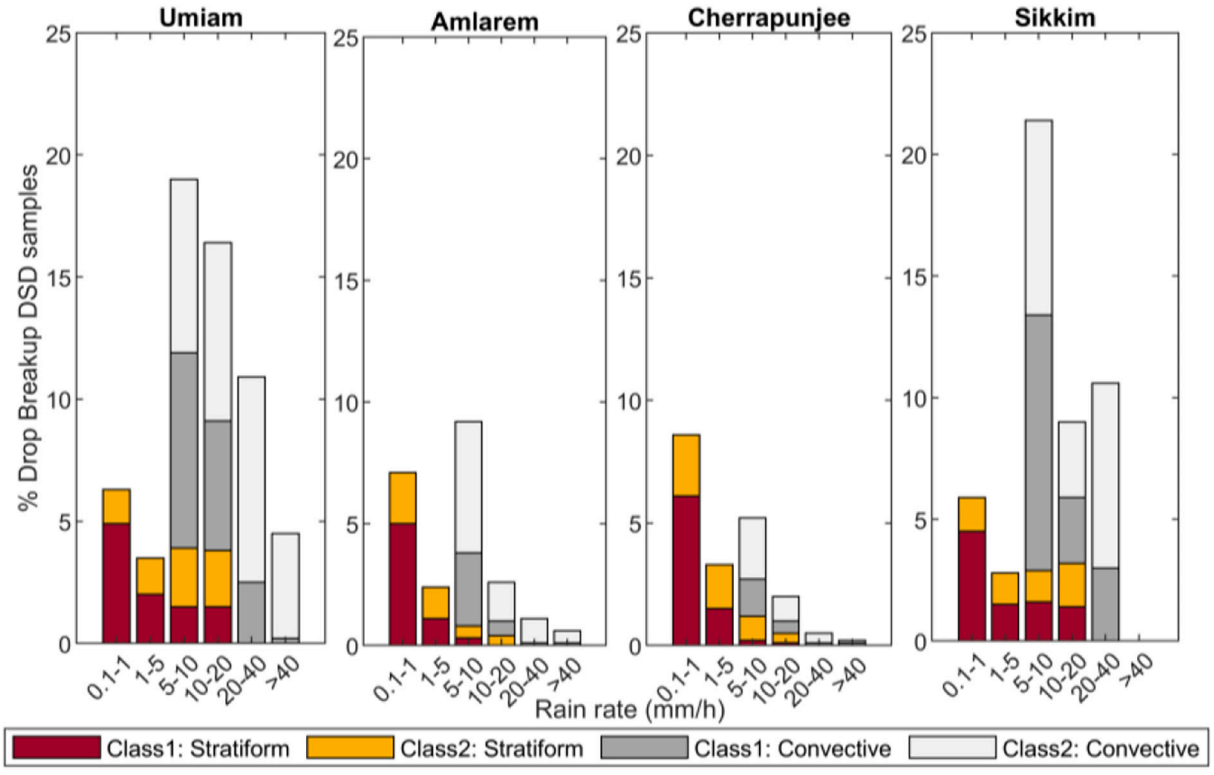

Fig. 11. Percentage occurrence of collisional drop breakup dominant classes (1 & 2) in all the HS Classes (1–6) with various rain intensity for each site location in Stratiform and Convective rain types.

comprehensive overview of the rainfall dynamics. Fig. 6 (b), shows the variations in rain intensity. Fig. 6 (c,d,e) illustrates the DSD for different classes with varied HS. As discussed in the methodology section, the breakup dominant DSD have a tendency to rise and make another peak between 1.0 and 2.6 mm diameter range which results in positive slope as shown in Fig. 6 (c, d). For class 1 (HS $\geq$ 0) which shows that

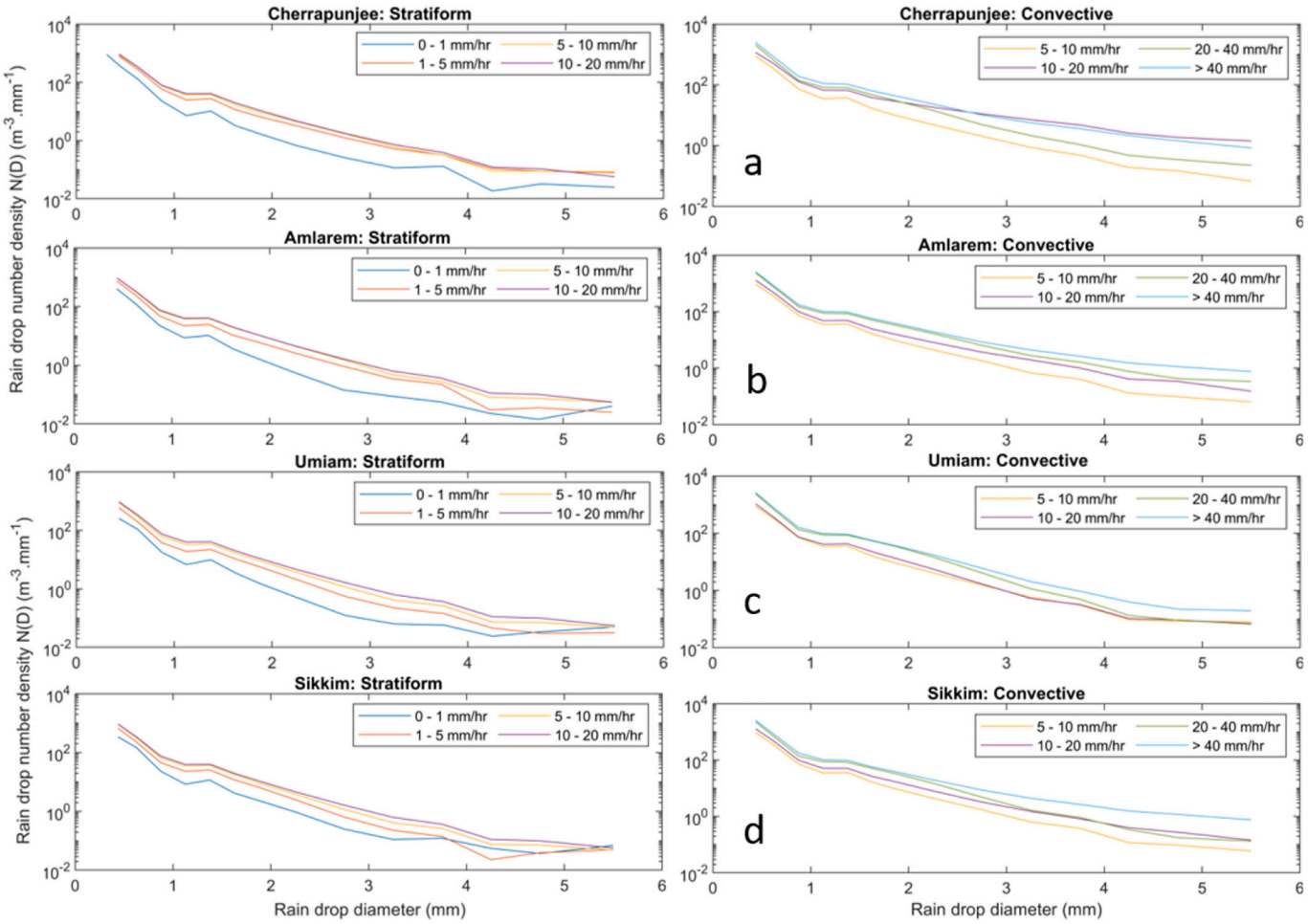

Fig. 12. Variation of mean DSDs in different rain intensity classes for stratiform and convective rain type over (a) Cherrapunjee, (b) Amlarem, (c) Umiam and (d) Sikkim.

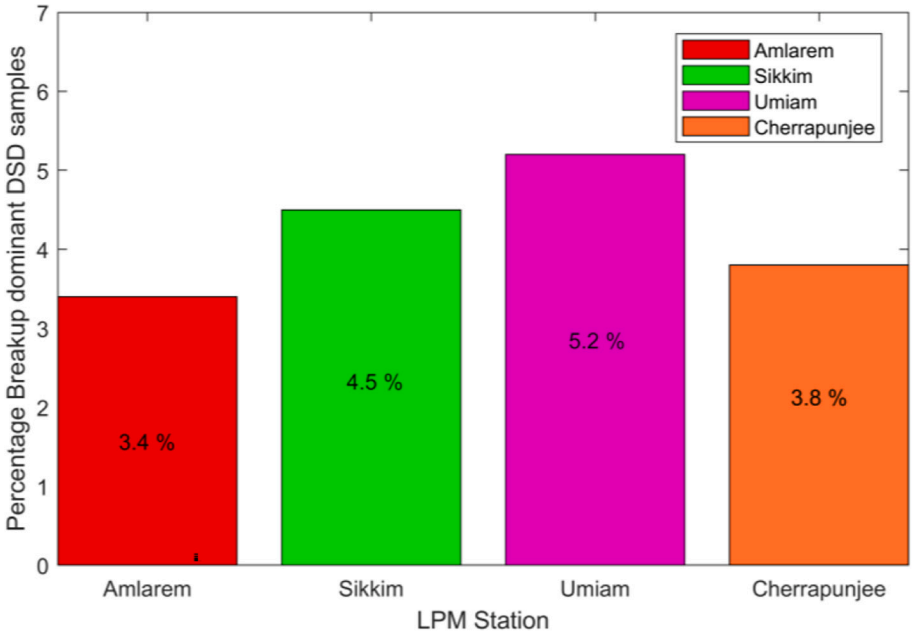

Fig. 13. Total combined percentage occurrence of breakup in the 2-min DSD samples for Umiam, Sikkim, Cherrapunjee and Amlarem.

Table 4
Z-R relationship coefficients A and b for each location and rain type sample.

	Umiam		Amlarem		Sikkim		Cherrapunjee	
	A	*b*	*A*	*b*	*A*	*b*	*A*	*b*
Convective Breakup (Non-Breakup)	459.20 (415.91)	1.151 (1.195)	442.60 (401.80)	1.411 (1.258)	377.57 (270.40)	1.283 (1.308)	654.64 (641.21)	1.373 (1.147)
Stratiform Breakup (Non-Breakup)	310.45 (174.60)	1.276 (1.316)	321.37 (175.0)	1.367 (1.331)	307.61 (167.11)	1.305 (1.312)	330.36 (178.64)	1.339 (1.327)

collisional breakup has happened and reached a balance, terming it equilibrium class. Class 2 ($-0.5 \leq HS < 0$) representing that equilibrium has not yet reached but the shape of the DSD has changed, thus classifying itself in the transitional class. Both class 1 and class 2 combinedly signifies the breakup dominant class. The DSD below -0.5 m^{-3} mm^{-2} are classified into non-breakup classes which constitutes four classes (class 3–6) with an interval of 0.5 m^{-3} mm^{-2} as shown in Fig. 6 (e)

In Fig. 7, mean DSDs for different HS classes have been shown. Notably, for the breakup-dominant classes (Class1 and Class2), the number concentration of raindrops decreased sharply until 0.875 mm and then gradually decrease up to 1.125 mm. Class 1 exhibited a more pronounced decrease in concentration compared to Class 2. Beyond 1.125 mm, both Class 1 and Class 2 showed an upward slope, leading to the observation of a second peak at 1.375 mm as seen in both Fig. 6 (c,d) as well in Fig. 7. Findings depicted in Fig. 7 highlights, that the inflection point, if observed, tends to occur within the range of 1–2.6 mm. This pattern remains consistent across different seasons, locations, and types of instruments. (Zawadzki and Antonio, 1988; Schlottke et al., 2010).

The breakup DSDs have positive HS values for comparatively low percentage of sample cases than other classes as shown in the Fig. 7. The low percentage of transitional class indicates that the majority of DSD doesn't have drop break up or the.

DSD already reaches an equilibrium. Amlarem shows the low percentage of equilibrium DSDs (2.0%) and Transitional DSDs (1.4%), indicating a lower occurrence of both equilibrium and transitional breakup compared to the other stations. The percentage equilibrium DSDs (2–4%) for all locations were slightly more than the transitional DSD percentage (1–2%).

These findings suggest that the majority of observed raindrops maintained their original size with minimal breakup. The observed variations in Class 1 and Class 2 percentages can be attributed to several factors. Geographic location and topography play a role, as each station is situated in a different location with unique weather patterns and atmospheric conditions. However, we haven't observed any notable dependence on the elevation on the drop break up statistics. It is to be noted though that with only a few locations, any conclusion on this topic is out of scope and needs further investigation. Microphysical processes within clouds, such as updraft strength, turbulence, and collisional processes, also influence raindrop behavior and subsequent breakup. Additionally, local meteorological conditions and precipitation intensity contribute to the variations, as higher precipitation rates are likely to increase the occurrence of raindrop collision and subsequent breakup.

3.2.2. Occurrences of collisional-drop breakup in rain intensity ranges

Figure 8 shows distribution of the number of 2-min samples of different HS classes with rain rate. It shows that the majority of distribution of the DSD samples are below the 6 mm/h rain intensity. Here, class 6 has a largest proportion of DSDs for all rain intensity compared to other classes. However, the combined breakup dominant classes substantially contribute to the natural orographic rain.

Table 3 Examines percentage occurrences of only drop breakup dominant classes (class 1 and class 2) in specific rain rate ranges for each location, it can be seen that the equilibrium DSDs (class 1) have the highest occurrence in the lowest rain rate range (0.1–1 mm/h) for all locations. The highest percentage is observed in Cherrapunjee (6.1%), followed by Amlarem (5.0%) and Sikkim (4.5%). Umiam has the lowest percentage of equilibrium DSDs (4.9%). Regarding the transitional DSDs (class 2) in the 0.1–1 mm/h rain rate range, the percentages range from 1.4% to 2.5%. Umiam has the highest occurrence of transitional DSDs (2.2%), followed by Sikkim (1.3%) and Amlarem (1.9%). Cherrapunjee has the lowest percentage of transitional DSDs (2.0%). This suggests that during light rainfall, a small portion of observations experience a transitional state between equilibrium and more pronounced negative slopes. This transitional behavior can arise from variations in atmospheric conditions or the presence of localized influences, leading to deviations from the equilibrium state (Longkumer et al., 2023). These values suggest that there is a notable presence of transitional DSDs within the 0.1–1 mm/h rain rate range. When excluding the 0.1–1 mm/h rain rate range for all locations, we find that the occurrence of equilibrium DSDs (class 1) generally decreases with increasing rain rate, while the occurrence of transitional DSDs (class 2) tends to increase. For class 1, the percentages range from approximately 1.2% to 2.0% for rain rates between 1 and 5 mm/h, and further decrease to about 0.4% to 2.1% for rain rates between 5 and 10 mm/h. In contrast, class 2 shows an increasing trend in percentage occurrence as rain rates increases. The percentages range from approximately 0.4% to 8.5% for rain rates between 20 and 40 mm/h, indicating a higher prevalence of transitional DSDs in heavier rainfall.

In Fig. 9, the distribution of DSD samples in different HS classes with rain rate ranges are shown. The higher occurrence of equilibrium DSDs (class 1) suggests a more consistent and stable rainfall regime, while the higher occurrence of transitional DSDs (class 2) indicates the presence of rainfall events with varying and drop size distributions. These statistics highlight the shifting distribution patterns of raindrop sizes in response to varying rain intensities, underscoring the dynamic nature of precipitation processes.

3.2.3. Collisional-drop breakup in stratiform and convective rain types

Figure 10 shows the combined percentage occurrences (3% - 5%) of breakup dominated DSDs in stratiform rain type which is almost similar for all locations. However, in convective rain, combined percentage occurrences of break up dominated samples are much less for Amlarem and Cherrapunjee (~2%) as compared to Sikkim and Umiam (9% -11%). It suggests that breakup in Sikkim and Umiam is majorly occurring in convective rain events whereas Amlarem and Cherrapunjee experiences breakup largely in stratiform rain. Another important result is that for Amlarem and Cherrapunjee, the occurrence of stratiform rain type is higher for class 1 DSD (2%–3%) and class 2 DSD (1%–2%) compared to the convective rain type (0.1%–2%) whereas the occurrence of class 1 DSD and class 2 DSD is higher in convective rain type (3.5%–4% and 5%–7% respectively) as compared to the stratiform rain type in class 1 and class2 DSD (3%–3.5% and 1%–2% respectively) for Sikkim and Umiam. This may be due to the fact that both the locations are situated nearby on the wind ward side and facing a vast Bangladesh plain area experiencing direct orography effect. As the warm moist air from Bay of Bengal travels toward the hills of Meghalaya. After reaching the hills of Meghalaya the moist air rises abruptly to a height of around 1400 m within a few kilometers distance. This process allows the water to condense rapidly and precipitate over the region. On the other hand, Sikkim is on a valley surrounded by hills and Umiam is on the Meghalaya plateau.

The Fig. 11 shows that while the specific proportions of class 1 and

class 2 may vary slightly among the locations, in general the class 1 (Equilibrium DSDs) is more dominant in stratiform rainfall, while class 2 (Transitional DSDs) is more prevalent in convective rainfall. In stratiform rain type for class 1 (0–1 mm/h), the percentage of collisional breakup is higher for all sites (Porcù et al., 2014). Although, collisional drop breakup may be influenced by both elevation and rain type simultaneously, but with only few locations measurements it was difficult to conclude about the elevation effect in the present study. This has to be explored further and will be taken as more data from other sites are available.

Furthermore, for the rain rate category of 5–10 mm/h, the highest breakup percentages were observed for all sites. This suggests that moderate rainfall intensity in the convective rain type contributes to enhanced collisional breakup processes, leading to a larger proportion of smaller raindrops. It is worth noting that for rain rates above 40 mm/h, the breakup percentage decreased significantly for all locations in class 2. This indicates that extremely heavy rainfall may have a suppressing effect on collisional breakup processes. In Fig. 12, DSDs of dominant breakup class (class 1 + class 2) for these two rain types are shown. All four locations in stratiform rain type had similar slopes of the mean DSDs.

3.2.4. Overall collisional-drop breakup in orographic rain regions

It is observed in the Fig. 13 that Amlarem has the lowest percentage of breakup dominant DSDs (3.4%), followed by Cherrapunjee (3.8%), Sikkim (4.5%), and Umiam (5.2%), thus location variation of drop breakup suggests that drop breakup is dominantly higher for Sikkim and Umiam, comparatively. The differences in topography, local climate patterns, and meteorological conditions could contribute to these variations. These statistics emphasize the importance of considering local factors and regional characteristics when studying rainfall patterns and their associated DSD classes. The variations in dominant DSD percentages highlight the complexity and uniqueness of rainfall characteristics in different locations, shedding light on the intricate interplay between meteorological factors and the raindrop size distribution.

3.3. Impact of collisional-drop breakup on Z-R relationship

The analysis indicate that a significant portion of the orographic rain undergoes collisional drop break-up. As the dynamics of drop size distribution plays a key role in the local rain micro-physics of the region, and subsequently on the rain integral parameters. Thus, the impact of collisional drop break up on retrieval of the rain rate in radar remote sensing need to be considered (Kumjian and Prat, 2014). The estimation of rain rate from radar reflectivity in weather radar relies on separate relationships for stratiform and convective rain. These relationships are often represented by the power law eq. $Z = AR^b$, where Z is the radar reflectivity in mm^6/m^3 and R is the rain rate in mm/h (Singh et al., 2023). The parameters 'b' (slope) and 'A' (intercept) in the equation depends on various factors such as location, terrain, rain type, and cloud structure (Das et al., 2011). The accurate determination of these equation parameters is crucial for improving the accuracy of rainfall estimation using radar reflectivity data.

Table 4 compares the coefficient values, showing the empirical coefficients are significantly separable for the two classes. Typically, a higher value of 'A' indicates convective weather conditions, while a lower value of 'A' suggests stratiform rain, which is also seen in our study, however, the results suggest that the intercept ('A') parameters for the *Z*-R relationships for breakup cases in all stations and rain types are higher than non-breakup cases. The slope ('b') parameter does not follow a definite pattern.

4. Conclusion

LPM datasets with approximately 113,205 two-minute averaged DSDs from four locations were analyzed to study the features of collisional drop breakup in orographic rain. The study showed that significant breakup occurred in both the equilibrium class (class 1) and the transitional class (class 2) for rain intensities ranging from 1 to 5 mm/h. The breakup percentage was highest for rain rates between 0.1 and 1 mm/h in class 1, and cumulatively, higher for low intensity rain (up to 5 mm/h) in a combined class 1 and class 2 in stratiform rain type. The breakup of raindrops was observed to be more significant for intermediate rain intensities in both stratiform and convective rain types. A notable breakup percentage in higher intensity rain was also observed.

The results also showed that when combining classes 1 and 2, the occurrence of breakup became substantial, with a higher percentage observed in convective samples (1% to 11%) compared to stratiform samples (4% to 5%). The proportion of raindrops falling into class 1 and class 2 DSDs differed for convective and stratiform rain types, but the combination of both classes represented a higher percentage overall. These findings confirm that the onset of equilibrium in collisional break up is a rare event in natural orographic rain. On the other hand, the breakup has a more significant impact in convective rain type in orographic rainfall patterns. The study also revealed location variations, with Sikkim and Umiam experiencing higher drop breakup percentages compared to Amlarem and Cherrapunjee. Furthermore, the occurrence of equilibrium DSD and transitional DSD was high in Amlarem and Cherrapunjee for stratiform rain types than convective rain types, while for Umiam and Sikkim, it was higher in convective rain types compared to stratiform rain types.

In this study, the *Z*-R relationship was also explored in both stratiform and convective rain types for breakup/non-breakup-based case samples. The results clearly showed that the Z-R relationship for breakup sample types is distinct from the Z-R relationship for non-breakup sample types. In rainy conditions where collisional drop breakup occurs, coefficient ('A') parameter for the Z-R relationship is higher across all stations and rain types. Notably, the slope ('b') parameter does not follow a definite pattern.

The study highlighted the significance of collisional breakup in shaping DSDs and its impact on radar-derived quantitative precipitation estimates (QPEs) in orographic rainfall regions. The study also calls for further research to deepen our understanding of the physical processes involved in collisional breakup and its implications for forecasting orographic rainfall and managing water resources in affected areas.

CRediT authorship contribution statement

Nitig Singh: Methodology, Formal analysis, Investigation, Data curation, Writing – original draft. **Saurabh Das:** Conceptualization, Methodology, Supervision, Writing – review & editing. **Udaya Kumar Sahoo:** Resources, Data curation. **Shyam Sundar Kundu:** Supervision, Conceptualization, Resources. **Swastika Chakraborty:** Resources, Data curation.

Declaration of competing interest

The authors declare no conflict-of-interest financial interest or personal relationship that could have appeared to influence the work reported in this work entitled "On Collisional Drop Breakup in Orographic Rain".

Data availability

Data from this study may be obtained from the corresponding authors upon request.

Acknowledgments

We thank the North Eastern Space Application Centre, Meghalaya and Sikkim Manipal Institute of Technology, Sikkim for providing Thies LPM measurements. Author (NS) thanks Dr. S. P. Aggarwal, Director

NESAC for providing the facility resources and support during field visits and Dr. Chandrani Chatterjee for her invaluable guidance. Authors (SC) also thankfully acknowledge the support under the ISRO-RESPOND program (ISRO/RES/3/790/18-19) for providing experimental facility. Author (SD) also thankfully acknowledge the financial support received under SERB (CRG/2022/006986) and MoES NARM(Moes/16/04/2021-RDESS/NARM-4) program.

References

Adirosi, Elisa, Porcu, Federico, Montopoli, Mario, Baldini, Luca, Bracci, Alessandro, Capozzi, Vincenzo, Annella, Clizia, Budillon, Giorgio, Bucchignani, Edoardo, Zollo, Alessandra, Cazzuli, O., Camisani, Giulio, Bechini, Renzo, Cremonini, Roberto, Antonini, Andrea, Ortolani, Alberto, Melani, Samantha, Valisa, Paolo, Scapin, Simone, 2023. Database of the Italian disdrometer network. Earth Syst. Sci. Data. 15, 2417–2429. https://doi.org/10.5194/essd-15-2417-2023.

Barthes, L., Mallet, C., 2023. Vertical evolution of raindrop size distribution: Impact on the shape of the DSD. Atmos. Res. 119 (13–22), 0169–8095. https://doi.org/10.1016/j.atmosres.2011.07.011.

Brazier-Smith, P.R., Jennings, S.G., Latham, J., 1972. The Interaction of Falling Water Drops: Coalescence. Proc. R. Soc. Lond. A 326 (1566), 393–408. https://doi.org/10.1098/rspa.1972.0016.

Bringi, V.N., Chandrasekar, V., Hubbert, J., Gorgucci, E., Randeu, W.L., Schoenhuber, M., 2003. Raindrop size distribution in different climatic regimes from disdrometer and dual-polarized radar analysis. J. Atmos. Sci. 60 (2), 354–365. https://doi.org/10.1175/1520-0469(2003)060<0354:RSDIDC>2.0.CO;2.

Caracciolo, C., Porcù, F., Prodi, F., 2008. Precipitation classification at mid-latitudes in terms of drop size distribution parameters. Adv. Geosci. 16 (11–17), 2008. https://doi.org/10.5194/adgeo-16-11-2008.

Chatterjee, C., Porcù, F., Das, S., Bracci, A., 2022. An Investigation on Super- and Sub-Terminal Drops in two different rain Categories and climate Regimes. Remote Sens. 14 (11), 2515. https://doi.org/10.3390/rs14112515.

Clima, Thies, 2022. Instructions for Use. Laser Precipitation Monitor 5.4110. xx. x00 V2. 7x STD. Available online: https://www.thiesclima.com/db/dnl/5.4110.xx.x00_Laser_Precipitation_Monitor_eng.pdf (accessed 01 January 2023).

Cotton, W.R., Gokhale, N.R., 1967. Collision, coalescence, and breakup of large water drops in a vertical wind tunnel. J. Geophys. Res. 72, 4041–4049. https://doi.org/10.1029/JZ072i016p04041.

D'Adderio, L.P., Porcù, F., Tokay, A., 2015. Identification and Analysis of Collisional Breakup in Natural rain. J. Atmos. Sci. 72, 3404–3416. https://doi.org/10.1175/JAS-D-14-0304.1.

D'Adderio, L.P., Porcù, F., Tokay, A., 2018. Evolution of drop size distribution in natural rain. Atmos. Res. 200, 70–76. ISSN 0169-8095,. https://doi.org/10.1016/j.atmosres.2017.10.003.

Das, S., Maitra, A., 2018. Characterization of tropical precipitation using drop size distribution and rain rate-radar reflectivity relation. Theor. Appl. Climatol. 132, 275–286. https://doi.org/10.1007/s00704-017-2073-1.

Das, S., Shukla, A.K., Maitra, A., 2009. Classification of convective and stratiform types of rain and their characteristics features at a tropical location. 2009. In: 4th International Conference on Computers and Devices for Communication (CODEC). Kolkata, India, pp. 1–4.

Das, S., Talukdar, Shamitaksha, Bhattacharya, Aniruddha, Adhikari, Arpita, Maitra, Animesh, 2011. Vertical profile of ZR relationship and its seasonal variation at a tropical location. In: In 2011 IEEE Applied Electromagnetics Conference (AEMC). IEEE, pp. 1–4. https://doi.org/10.1109/AEMC.2011.6256915.

Gillespie, J.R., List, R., 1978. Effects of collision-induced breakup on drop size distributions in steady state rainshafts. Pure Appl. Geophys. PAGEOPH 117 (4), 599–626. https://doi.org/10.1007/BF00879971.

Houze, R.A., 1993. Cloud Dynamics. International Geophysics Series, Vol. 53. Academic Press, p. 573.

Houze, R.A., 1997. Stratiform precipitation in regions of convection: a meteorological paradox? Bull. Am. Meteor. Soc. 78, 2179–2196.

Johannsen, L.L., Zambon, N., Strauss, P., Dostal, T., Neumann, M., Zumr, D., Cochrane, T.A., Blöschl, G., Klik, A., 2020. Comparison of three types of laser optical disdrometers under natural rainfall conditions. Hydrol. Sci. J. 65 (4), 524–535. https://doi.org/10.1080/02626667.2019.1709641.

Johnson, D.B., 1982. Raindrop multiplication by drop breakup. J. Appl. Meteorol. Climatol. 21, 1048–1050. https://doi.org/10.1175/1520-0450(1982)021<1048:RMBDB>2.0.CO;2.

Kadiri, S., Radhakrishna, B., Rao, T.N., 2023. Seasonal differences in raindrop size and causative microphysical processes in continental, orographic and oceanic regions of the Indian subcontinent. Atmos. Res. 281, 106501 https://doi.org/10.1016/j.atmosres.2022.106501.

Kalita, R., Kalita, D., Saxena, A., 2021. Trends in Extreme Climate Indices in Cherrapunjee for the Period 1979 to 2020. Doi:10.21203/rs.3.rs-706445/v1.

Konwar, M., Raut, B.A., Rao, Y.J., Prabhakaran, T., 2022. Rain microphysical properties over the rain shadow region of India. Atmos. Res. 275 (106224), 0169–8095. https://doi.org/10.1016/j.atmosres.2022.106224.

Kumjian, M., Prat, O., 2014. The impact of raindrop collisional processes on the polarimetric radar variables. J. Atmos. Sci. 71, 3052–3067. https://doi.org/10.1175/JAS-D-13-0357.1.

Kundu, A., Kundu, S.S., Sharma, S.K., Gogoi, M., Banik, T., Borgohain, A., Mahanta, R., Debnath, A., 2023. The behavior of cloud base height over a hilly remote station of North-East India using ground-based remote sensing technique. Atmos. Res. 282 (106512), 0169–8095. https://doi.org/10.1016/j.atmosres.2022.106512.

List, R., Gillespie, J.R., 1976. Evolution of raindrop spectra with collision-induced breakup. J. Atmos. Sci. 33, 2007–2013. https://doi.org/10.1175/1520-0469(1976)033<2007:EORSWC>2.0.CO;2.

Longkumer, I., Biswasharma, R., Pongener, I., Roy, P., Samanta, D., Konwar, M., Sharma, S., 2023. A study of rain drop size distributions and associated rain microphysical processes over a subtropical station in the Northeast India. J. Atmos. Sol.-Terr. Phy. 247 (106073), 1364–6826. https://doi.org/10.1016/j.jastp.2023.106073.

Low, T.B., List, R., 1982. Collision, coalescence and breakup of raindrops. Part I: Experimentally established coalescence efficiencies and fragment size distributions in breakup. J. Atmos. Sci. 39, 1591–1606. https://doi.org/10.1175/1520-0469(1982)039,1591:CCABOR.2.0.CO;2.

McFarquhar, G.M., 2004. A new representation of collision-induced breakup of raindrops and its implications for the shapes of raindrop size distributions. J. Atmos. Sci. 61 (7), 777–794. https://doi.org/10.1175/1520-0469(2004)061<0777:ANROCB>2.0.CO;2.

Murata, F., Terao, T., Chakravarty, K., Syiemlieh, H.J., Cajee, L., 2020. Characteristics of orographic rain drop-size distribution at Cherrapunjee, Northeast India. Atmosphere 11 (8), 777. https://doi.org/10.3390/atmos11080777.

Pickering, B.S., Neely III, R.R., Harrison, D., 2019. The Disdrometer Verification Network (DiVeN): a UK network of laser precipitation instruments. Atmos. Meas. Tech. 12, 5845–5861. https://doi.org/10.5194/amt-12-5845-2019.

Porcù, F., D'Adderio, L.P., Prodi, F., Caracciolo, C., 2013. Effects of altitude on maximum raindrop size and fall velocity as limited by collisional breakup. J. Atmos. Sci. 70, 1129–1134. https://doi.org/10.1175/JAS-D-12-0100.1.

Porcù, F., D'Adderio, L.P., Prodi, F., Caracciolo, C., 2014. Rain drop size distribution over the Tibetan Plateau. Atmos. Res. 150 (21–30), 0169–8095. https://doi.org/10.1016/j.atmosres.2014.07.005.

Pruppacher, H.R., Klett, J.D., Wang, P.K., 1980. Microphysics of Clouds and Precipitation. Aerosol Sci. Technol. 28, 381–382.

Radhakrishna, B., Narayana Rao, T., 2009. Statistical characteristics of Multipeak Raindrop size distributions at the Surface and aloft in different rain Regimes. Mon. Weather Rev. 137, 3501–3518. https://doi.org/10.1175/2009MWR2967.1.

Saikranthi, K., Radhakrishna, B., Rao, T.N., 2023. Seasonal differences in raindrop size and causative microphysical processes in continental, orographic and oceanic regions of the Indian subcontinent. Atmos. Res. 281 (106501), 0169–8095. https://doi.org/10.1016/j.atmosres.2022.106501.

Schlottke, J., Straub, W., Beheng, K., Gomaa, H., Weigand, B., 2010. Numerical investigation of collision-induced breakup of raindrops. Part I: methodology and dependencies on collision energy and eccentricity. J. Atmos. Sci. 67, 557–575. https://doi.org/10.1175/2009JAS3174.1.

Singh, N., Tyagi, V., Das, S., Sahoo, U.K., Kundu, S.S., 2023. Investigation of Orographic Z-R Relationships for Three Locations in India," 2023 XXXVth General Assembly and Scientific Symposium of the. International Union of Radio Science (URSI GASS, Sapporo, Japan, pp. 1–4. https://doi.org/10.23919/URSIGASS57860.2023.10265609.

Testik, F.Y., Barros, A.P., Bliven, L.F., 2011. Toward a physical characterization of raindrop collision outcome regimes. J. Atmos. Sci. 68 (5), 1097–1113.

Tokay, A., Short, D.A., 1996. Evidence from tropical raindrop spectra of the origin of rain from stratiform versus convective clouds. J. Appl. Meteorol. 35, 355–371. https://doi.org/10.1175/1520-0450(1996)035<0355:EFTRSO>2.0.CO;2.

Tokay, A., Petersen, W.A., Gatlin, P., Wingo, M., 2013. Comparison of raindrop size distribution measurements by collocated disdrometers. J. Atmos. Ocean. Technol. 30 (8), 1672–1690. https://doi.org/10.1175/JTECH-D-12-00163.1.

Valdez, M.P., Young, K.C., 1985. Number fluxes in equilibrium raindrop populations: a Markov chain analysis. J. Atmos. Ocean. Technol. 2, 829–839.

Zawadzki, I., Antonio, M.D.A., 1988. Equilibrium raindrop size distributions in tropical rain. J. Atmos. Sci. 45, 3452–3459. https://doi.org/10.1175/1520-0469(1988)045,3452: ERSDIT.2.0.CO;2.

Zeng, Y., Yang, L., Zhou, Y., Tong, Z., Jiang, Y., Chen, P., 2022. Characteristics of orographic raindrop size distribution in the Tianshan Mountains, China. Atmos. Res. 278 (106332), 0169–8095. https://doi.org/10.1016/j.atmosres.2022.106332.